

Contents lists available at [SciVerse ScienceDirect](http://SciVerse.ScienceDirect.com)

Physics Letters B

www.elsevier.com/locate/physletb

Discrimination of models including doubly charged scalar bosons by using tau lepton decay distributions

Hiroaki Sugiyama^a, Koji Tsumura^{b,*}, Hiroshi Yokoya^{c,d,1}

^a Department of Physics, University of Toyama, Toyama 930-8555, Japan

^b Department of Physics, Graduate School of Science, Nagoya University, Nagoya 464-8602, Japan

^c Department of Physics and Center for Theoretical Sciences, National Taiwan University, Taipei 10617, Taiwan

^d National Center for Theoretical Sciences, National Taiwan University, Taipei 10617, Taiwan

ARTICLE INFO

Article history:

Received 30 June 2012

Received in revised form 14 September 2012

Accepted 18 September 2012

Available online 24 September 2012

Editor: T. Yanagida

Keywords:

Doubly charged Higgs boson

Tau lepton polarization

ABSTRACT

The doubly charged scalar boson ($H^{\pm\pm}$) is introduced in several models of the new physics beyond the standard model. The $H^{\pm\pm}$ has Yukawa interactions with two left-handed charged leptons or two right-handed charged leptons depending on the models. We study kinematical properties of $H^{\pm\pm}$ decay products through tau leptons in order to discriminate the chiral structures of the new Yukawa interaction. The chirality of tau leptons can be measured by the energy distributions of the tau decay products, and thus the chiral structure of the new Yukawa interaction can be traced in the invariant-mass distributions of the $H^{\pm\pm}$ decay products. We perform simulation studies for the typical decay patterns of the $H^{\pm\pm}$ with simple event selections and tau-tagging procedures, and show that the chiral structure of the Yukawa interactions of $H^{\pm\pm}$ can be distinguished by measuring the invariant-mass distributions.

© 2012 Elsevier B.V. Open access under [CC BY license](http://creativecommons.org/licenses/by/3.0/).

1. Introduction

The existence of the neutrino masses has been established well [1–6]. However, neutrinos are massless in the standard model (SM) because of the absence of the right-handed partners. If the lepton number conservation is violated in a new physics model beyond the SM, neutrinos can be Majorana particles which form a mass term with its self-conjugation field only [7], since neutrinos are electrically neutral unlike to all other SM fermions. Therefore, it seems natural to expect that the possible Majorana nature of neutrinos provides the reason why neutrinos have very different masses from those of other SM fermions.

The doubly charged scalar boson H^{--} , which has a twice electrical charge of the electron, exists in several models to generate Majorana neutrino masses. For instance, the particle is a member of an $SU(2)_L$ triplet scalar field in the Higgs triplet model (HTM) [8]. The triplet field develops a tiny vacuum expectation value (VEV), which breaks the lepton number conservation and is the source of the neutrino mass. Such a triplet field appears also in some models of extended gauge symmetries [9]. On

the other hand, a doubly charged scalar boson is introduced as an $SU(2)_L$ singlet scalar field in the Zee–Babu model (ZBM) [10] which generates Majorana neutrino masses at the two-loop level. In these models with H^{--} , its Yukawa interactions with charged leptons depend on the $SU(2)_L$ property of H^{--} . Namely, H^{--} from an $SU(2)_L$ triplet field couples only with left-handed charged leptons ℓ_L^- while the one from an $SU(2)_L$ singlet field interacts only with right-handed charged leptons ℓ_R^- . Furthermore, H^{--} can be a component of other $SU(2)_L$ multiplet scalars [11], and such H^{--} also has Yukawa interactions with two left-handed or two right-handed charged leptons through the mixings between leptons and new fermions. In any case, both of two charged leptons which couple with H^{--} via the Yukawa interaction are left-handed or right-handed. The discrimination of the chiral structure of the Yukawa interaction plays an important role to distinguish these models.

The $H^{\pm\pm}$ can be produced by the pair creation process, $pp \rightarrow \gamma^*/Z^* \rightarrow H^{++}H^{--}$. For $SU(2)_L$ non-singlet representations, the associated production $pp \rightarrow W^{\mp*} \rightarrow H^{\pm}H^{\mp\mp}$ with a singly charged scalar boson (H^{\pm}) is also possible [12]. Theoretical studies for $H^{\pm\pm}$ decaying into same-signed leptons and weak gauge bosons can be found in, e.g., Refs. [13,14]. The experimental search results for $H^{\pm\pm}$ have been available, where purely leptonic decay channels are assumed [15–17]. We comment that these bounds on the $H^{\pm\pm}$ mass are dependent on the production mechanism, the decay branching ratios, and the mass spectrum of the scalar boson multiplets [18].

* Corresponding author.

E-mail addresses: sugiyama@sci.u-toyama.ac.jp (H. Sugiyama), ko2@eken.phys.nagoya.ac.jp (K. Tsumura), hyokoya@hep1.phys.ntu.edu.tw (H. Yokoya).

¹ Address after September 2012: Department of Physics, University of Toyama, Toyama 930-8555, Japan.

In this Letter, we study the consequence of the chiral structure of the Yukawa interaction (of the doubly charged scalar boson with two charged leptons) to the kinematical distribution involving the decay of tau leptons. The polarization of τ leptons is known to be probed by its decay products, and can be exploited to test the structure of new interactions in the models beyond the SM [19–21]. In Section 2, models of neutrino masses with $H^{\pm\pm}$ are introduced with particular attention to the chiral structure of the Yukawa interaction. In Section 3, the polarization dependences of the decay distributions of τ leptons are reviewed, and the invariant-mass distributions of final-state particles in the decay of $H^{\pm\pm}$ into at least one τ lepton are discussed. Simulation results including τ -tagging and simple kinematical cuts are also presented. Conclusions are given in Section 4.

2. Models with doubly charged scalar bosons

In this section, we briefly present examples of models which include the doubly charged scalar boson.

The first example is the HTM [8]. In this model, an $SU(2)_L$ adjoint scalar field Δ with hypercharge $Y = 1$ is introduced in order to generate masses of neutrinos via the triplet Yukawa interaction. The new Yukawa interaction is given by

$$\mathcal{L}_{\text{HTM}}^{\text{Yukawa}} = -\bar{L}^c h_M i \sigma_2 \Delta L + \text{H.c.}, \quad (1)$$

where $L = (\nu_L, \ell_L^-)^T$ is the lepton doublet field, the Yukawa coupling matrix is symmetric $h_M = h_M^T$, $\sigma_i (i = 1-3)$ are the Pauli matrices, and

$$\Delta = \begin{pmatrix} \Delta^+/\sqrt{2} & \Delta^{++} \\ \Delta^0 & -\Delta^+/\sqrt{2} \end{pmatrix}. \quad (2)$$

In the HTM, the doubly charged scalar boson interacts with a pair of *left-handed* charged leptons. The neutrino mass matrix in the flavor basis is obtained as $M_\nu^{\text{HTM}} = 2h_M^\dagger \langle \Delta^0 \rangle = U_{\text{MNS}} \hat{M}_\nu U_{\text{MNS}}^T$, where $\langle \Delta^0 \rangle$ is the VEV of the triplet field, \hat{M}_ν is the neutrino mass matrix in the diagonal basis, and U_{MNS} is the Maki–Nakagawa–Sakata (MNS) matrix for the lepton flavor mixing. Since the neutrino mass matrix is directly related to the Yukawa matrix, the decay patterns of the doubly charged scalar boson are constrained by observed neutrino oscillation data [22]. For example, $(h_M)_{\mu\mu} \approx (h_M)_{\tau\tau}$ and $(h_M)_{e\mu} \approx (h_M)_{e\tau}$ are required because the observed neutrino mass matrix approximately has the μ - τ exchange symmetry. By assuming the realistic values of decay branching ratios, constraints on the mass of $\Delta^{\pm\pm}$ are obtained as $m_{\Delta^{\pm\pm}} \gtrsim 400$ GeV [16].

The next example is the ZBM [10]. Two $SU(2)_L$ singlet scalar bosons, $k^- (Y = -1)$ and $k^{--} (Y = -2)$, are introduced in the ZBM to generate tiny neutrino masses at the two-loop level. The new interaction terms which relevant to the radiative neutrino mass are

$$\mathcal{L}_{\text{ZBM}} = -\bar{L}^c Y_a i \sigma_2 L k^+ - \overline{(\ell_R^-)^c} Y_s \ell_R^- k^{++} - \mu k^- k^- k^{++} + \text{H.c.}, \quad (3)$$

where $Y_a = -Y_a^T$ and $Y_s = Y_s^T$. The doubly charged scalar boson in this model interacts with *right-handed* charged leptons. If a lepton number 2 is assigned to k^- and k^{--} , a coupling constant μ is the soft breaking parameter of the lepton number conservation. The neutrino mass matrix is calculated as $(M_\nu^{\text{ZBM}})_{\alpha\beta} = 16\mu(Y_a^*)_{\alpha\ell} m_\ell (Y_s)_{\ell\ell'} I_{\ell\ell'} m_{\ell'} (Y_a^\dagger)_{\ell'\beta}$, where the loop function $I_{\ell\ell'}$ is given in Ref. [23]. In order to describe the observed neutrino oscillation parameters, $(Y_s)_{\mu\mu} (m_\mu/m_\tau)^2 \sim (Y_s)_{\mu\tau} (m_\mu/m_\tau) \sim (Y_s)_{\tau\tau}$ is favored in the ZBM [24]. This may suggest that $k^{--} \rightarrow \tau_R^- \tau_R^-$ would be highly suppressed while $k^{--} \rightarrow \mu_R^- \tau_R^-$ could be sizable

in the ZBM. Assuming purely muonic decay mode, the mass of $k^{\pm\pm}$ is constrained to be $m_{k^{\pm\pm}} \gtrsim 250$ GeV [17].²

3. Tau polarizations and doubly charged scalar boson decays

3.1. Decay distributions of polarized tau leptons

In this section, we review the polarization dependence of decays of τ 's, and discuss how that could be traced in the case of $H^{\pm\pm}$ decay through τ 's. In the following discussion, we assume that the leptonic decays of doubly charged scalar bosons occur via the Yukawa interactions, e.g., $H_X^- \bar{\ell}_X (\tau_X)^c$ ($X = L, R$), where $H_L^- (H_R^-)$ denotes H^{--} only with the left-handed (right-handed) interaction. Hereafter, ℓ denotes e or μ .

First, let us consider the lepton flavor violating (LFV) decay $H^{--} \rightarrow \ell^- \tau^-$ followed by $\tau^- \rightarrow \pi^- \nu$. The branching ratio of the pionic decay of τ is about 11% while the branching ratio of the total hadronic decay is about 65%. The invariant-mass of $\ell\pi$ is expressed as $M_{\ell\pi}^2 = z m_{H^{\pm\pm}}^2$ in the collinear limit, where $m_{H^{\pm\pm}}$ is the mass of $H^{\pm\pm}$ and $z \equiv E_\pi/E_\tau$; the E_π and E_τ are energies of a pion and a τ lepton in the laboratory frame, respectively. This relation between the invariant-mass and the energy fraction is a good approximation for an energetic τ lepton, e.g., a τ lepton produced by a heavy particle decay.

The distributions of the pion energy fraction z (namely, of the invariant-mass $M_{\ell\pi}^2$) are given as

$$\mathcal{D}_L^\pi(z) = F_L^\pi(z) = 2(1-z), \quad (4a)$$

$$\mathcal{D}_R^\pi(z) = F_R^\pi(z) = 2z, \quad (4b)$$

where $F_{L,R}^\pi(z)$ are the fragmentation functions of $\tau_{L,R}^- \rightarrow \pi^- \nu$ decay in the collinear limit [19]. The fragmentation functions for the other hadronic decay modes are also known but less sensitive to the polarization of τ [19]. We will utilize these decay modes in the simulation study later.

When the LFV decay is followed by the leptonic decays of τ 's, the dilepton invariant-mass is expressed as $M_{\ell\ell'}^2 = z m_{H^{\pm\pm}}^2$ in the collinear limit, where z is the energy fraction of the daughter lepton to the parent τ lepton. We denote ℓ_τ^\pm as ℓ^\pm from decays of τ^\pm .³ The total branching ratio of the leptonic decays is about 35%. The distributions of z (namely, of $M_{\ell\ell'}^2$) are given as

$$\mathcal{D}_L^\ell(z) = F_L^\ell(z) = \frac{4}{3}(1-z^3), \quad (5a)$$

$$\mathcal{D}_R^\ell(z) = F_R^\ell(z) = 2(1-z)^2(1+2z), \quad (5b)$$

where $F_{L,R}^\ell(z)$ are the fragmentation functions of $\tau_{L,R}^- \rightarrow \ell^- \nu$ decay in the collinear limit [19].

In Fig. 1, we plot the distributions of the invariant-masses of $\ell\pi$ (left panel) and $\ell\ell_\tau$ (right panel) for the LFV decay $H^{--} \rightarrow \ell^- \tau^-$ followed by the pionic and leptonic decays of the τ , respectively. The invariant-mass distributions via the decay of τ_L (τ_R) are plotted in the dashed (solid) curves. For the pionic decay channel, the distributions are linear in z and have an opposite behavior between τ_L and τ_R . On the other hand, the right panel of Fig. 1 shows that the distribution of $M_{\ell\ell_\tau}$ for the leptonic τ decay would be less sensitive to the τ polarization than that of the pionic channel.

² If we use theoretical curves in Fig. 2 of Ref. [17] with the result of Ref. [16] ($m_{\Delta^{\pm\pm}} > 391$ GeV for pair-produced $\Delta^{\pm\pm}$ with the 100% decay branching ratio into a muon pair), we would naively arrive at $m_{k^{\pm\pm}} \gtrsim 320$ GeV.

³ The notation $\ell_{(\tau)}\ell_{(\tau)}$ indicates not only ee and $\mu\mu$ but also $e\mu$.

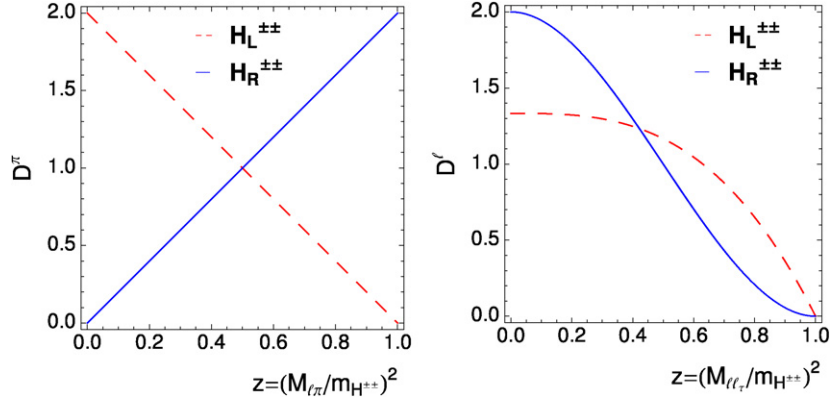


Fig. 1. Distributions of the invariant-mass of $\ell\pi$ (left panel) and of $\ell\ell$ (right panel) from the LFV decay $H^{--} \rightarrow \ell^-\tau^-$, where $\ell_{(\tau)} = e, \mu$. The invariant-mass distributions through the decay of τ_L (τ_R) are plotted in the dashed (solid) curves.

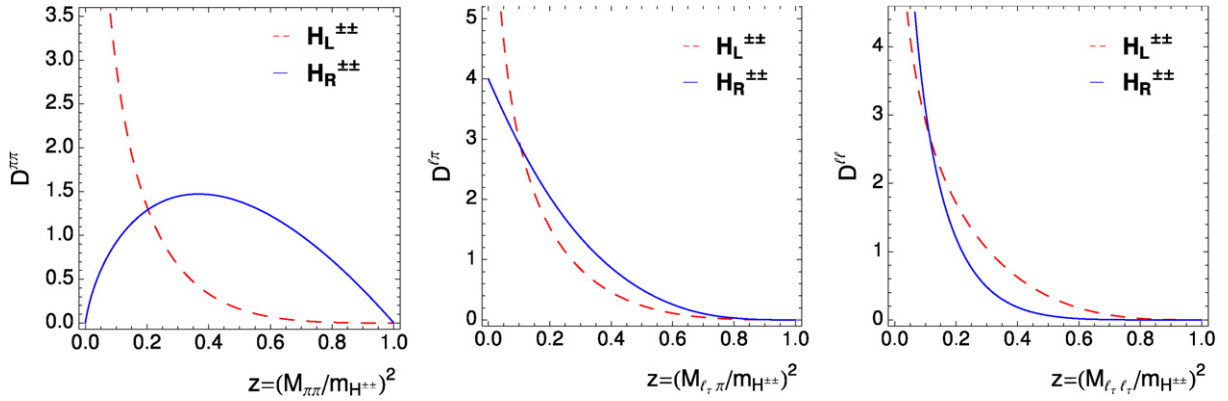


Fig. 2. Distributions of the invariant-mass of $\pi\pi$ (left panel), $\ell_t\pi$ (middle panel) and of $\ell_t\ell_t$ (right panel) from $H^{--} \rightarrow \tau^-\tau^-$, where $\ell_t = e, \mu$. The invariant-mass distributions through the decay of τ_L (τ_R) are plotted in the dashed (solid) curves.

Next, we consider the decay mode $H^{--} \rightarrow \tau^-\tau^-$. The decay pattern of the two τ 's can be classified into three categories: hadronic channels (e.g. $\pi\pi$), semi-leptonic channels (e.g. $\ell_t\pi$), and purely leptonic channels ($\ell_t\ell_t$). The distributions of $\pi\pi$ invariant-mass $M_{\pi\pi}$ in $H^{--} \rightarrow \tau^-\tau^- \rightarrow \pi^-\pi^-\nu\bar{\nu}$ decay chain are calculated by convoluting the fragmentation functions of the pionic decays of τ 's in Eqs. (4) as follows [21]:

$$\begin{aligned} \mathcal{D}_{LL}^{\pi\pi}(z) &= \int_z^1 \frac{dz_1}{z_1} F_L^\pi(z_1) F_L^\pi(z/z_1) \\ &= 4 \left[(1+z) \log \frac{1}{z} + 2z - 2 \right], \end{aligned} \quad (6a)$$

$$\mathcal{D}_{RR}^{\pi\pi}(z) = \int_z^1 \frac{dz_1}{z_1} F_R^\pi(z_1) F_R^\pi(z/z_1) = 4z \log \frac{1}{z}, \quad (6b)$$

where $z = M_{\pi\pi}^2/m_{H^{++}}^2$ in the collinear limit and $\mathcal{D}_{LL}^{\pi\pi}$ ($\mathcal{D}_{RR}^{\pi\pi}$) is the distribution for $H_L^{\pm\pm}$ ($H_R^{\pm\pm}$).

The distributions of the $\ell_t\pi$ invariant-mass $M_{\ell_t\pi}$ for the $H^{--} \rightarrow \tau^-\tau^- \rightarrow \ell_t^-\pi^-\nu\bar{\nu}$ decay chain are given by

$$\begin{aligned} \mathcal{D}_{LL}^{\ell_t\pi}(z) &= \int_z^1 \frac{dz_1}{z_1} F_L^{\ell_t}(z_1) F_L^\pi(z/z_1) \\ &= \frac{4}{9} \left[6 \log \frac{1}{z} - z^3 + 9z - 8 \right], \end{aligned} \quad (7a)$$

$$\mathcal{D}_{RR}^{\ell_t\pi}(z) = \int_z^1 \frac{dz_1}{z_1} F_R^{\ell_t}(z_1) F_R^\pi(z/z_1) = 4(1-z)^3, \quad (7b)$$

where $z = M_{\ell_t\pi}^2/m_{H^{++}}^2$ in the collinear limit. The distribution $\mathcal{D}_{LL}^{\ell_t\ell_t}$ ($\mathcal{D}_{RR}^{\ell_t\ell_t}$) is for $H_L^{\pm\pm}$ ($H_R^{\pm\pm}$).

The dilepton invariant-mass distributions for the $H^{--} \rightarrow \tau^-\tau^- \rightarrow \ell_t^-\ell_t^-\nu\bar{\nu}$ decay chain are given by

$$\begin{aligned} \mathcal{D}_{LL}^{\ell_t\ell_t}(z) &= \int_z^1 \frac{dz_1}{z_1} F_L^{\ell_t}(z_1) F_L^{\ell_t}(z/z_1) \\ &= -\frac{16}{27} \left[2 - 2z^3 - 3(1+z^3) \log \frac{1}{z} \right], \end{aligned} \quad (8a)$$

$$\begin{aligned} \mathcal{D}_{RR}^{\ell_t\ell_t}(z) &= \int_z^1 \frac{dz_1}{z_1} F_R^{\ell_t}(z_1) F_R^{\ell_t}(z/z_1) \\ &= \frac{4}{3} \left[-5 - 27z^2 + 32z^3 \right. \\ &\quad \left. + 3(1+9z^2+4z^3) \log \frac{1}{z} \right], \end{aligned} \quad (8b)$$

where $z = M_{\ell_t\ell_t}^2/m_{H^{++}}^2$ in the collinear limit and $\mathcal{D}_{LL}^{\ell_t\ell_t}$ ($\mathcal{D}_{RR}^{\ell_t\ell_t}$) is for $H_L^{\pm\pm}$ ($H_R^{\pm\pm}$).

In Fig. 2, we plot the distributions of the invariant-mass of $\pi\pi$ (left panel), $\ell_t\pi$ (middle panel), and $\ell_t\ell_t$ (right panel) from

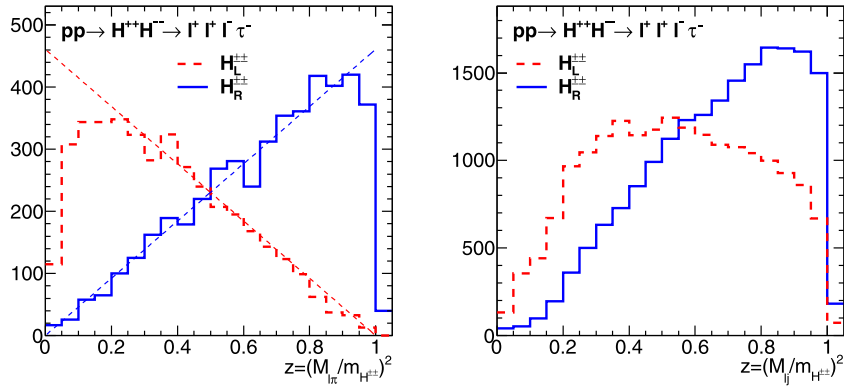


Fig. 3. Invariant-mass distributions of $\ell\pi\tau$ (left) and ℓj_τ (right) in the $pp \rightarrow H^{++}H^{--} \rightarrow \ell^+\ell^+\ell^-\tau^-$ process followed by hadronic decays of τ^- , after the requirement of the same-signed dilepton with $M_{\ell\ell} \simeq m_{H^{\pm\pm}}$. Dashed (solid) histograms are for $H_L^{\pm\pm}$ ($H_R^{\pm\pm}$). Smooth lines in the left panel are theoretical expectations by using Eqs. (4) with some normalization.

$H^{--} \rightarrow \tau^-\tau^-$. The invariant-mass distributions through the decay of τ_L (τ_R) are plotted in the dashed (solid) curves. Owing to the large polarization dependence of the pionic decay fragmentation function in Eqs. (4), the $\pi\pi$ invariant-mass distribution has a large power for the spin analysis. Namely, the distribution takes a large value in the region of a small z for the $H_L^{\pm\pm}$ decay while it is large for $z \simeq 0.4$ in the $H_R^{\pm\pm}$ decay. The $\ell_\tau\pi$ and $\ell_\tau\ell_\tau$ distributions in the middle and right panels of Fig. 2, respectively, take a large value for a small z for both $H_R^{\pm\pm}$ and $H_L^{\pm\pm}$, thus are not useful as the τ polarization discriminator.

To summarize, the invariant-mass distributions of $\ell\pi$ (and $\ell\ell_\tau$) in the $H^{--} \rightarrow \ell^-\tau^-$ decay and $\pi\pi$ in the $H^{--} \rightarrow \tau^-\tau^-$ decay are good for discriminating the τ polarization and thus the chiral structure of the Yukawa interaction with $H^{\pm\pm}$. Notice that the $\ell\pi$ ($\ell\ell$) final-state can be reached through the other decay chain(s) such like $H^{--} \rightarrow \tau^-\tau^- \rightarrow \ell_\tau^-\pi^-\nu\nu$ ($H^{--} \rightarrow \ell^-\ell^-$ and $H^{--} \rightarrow \tau^-\tau^- \rightarrow \ell_\tau^-\ell_\tau^-\nu\nu$). If these decay modes for $H^{\pm\pm}$ exist simultaneously, the signatures from these decay chains would mix in general. It should be possible to treat the mixed signatures or to divide them by kinematical cuts. However, since such analyses depend on the detail branching ratio of the $H^{\pm\pm}$ decay, we will not consider them in this study.

3.2. Simulation results

In order to perform realistic studies for collider experiments, we examine a Monte-Carlo simulation for the $H^{++}H^{--}$ pair production and their decays up to parton-showering and hadronizations. We generate signal events of $pp \rightarrow H^{++}H^{--}$ by using Pythia [25] with handling the τ decay by TAUOLA [26] incorporating the chiral properties of the Yukawa interactions of $H^{\pm\pm}$. We consider only the leptonic decay of $H^{\pm\pm}$, and pick up several patterns of the pair of decays suited for the τ polarization measurement. The $m_{H^{\pm\pm}}$ is set to be 400 GeV, and the collider energy to $\sqrt{s} = 14$ TeV. For the reference, the $H^{++}H^{--}$ production cross-sections is 4.6 fb for the HTM and 1.9 fb for the ZBM. For the analysis, we use lighter leptons (e and μ) with $p_T^\ell > 15$ GeV and $|\eta_\ell| < 2.5$, where p_T is the transverse momentum and η is the pseudo rapidity. To find the hadronically decaying τ 's, we perform τ -tagging for every jets with $p_T^j > 25$ GeV and $|\eta_j| < 2.5$ which are constructed by the anti- k_T algorithm [27] with $R = 0.4$. For the τ -tagging, we use two methods. The first method is devoted to extract the $\tau \rightarrow \pi\nu$ decay. Namely, it is tagged as the pionic τ -jet (π_τ) if a jet has only 1 charged hadron and its transverse energy dominates more than 0.95 of the jet. The second method is a more general-purpose; we define j_τ as a jet which contains 1 or 3 charged tracks in a small cone ($R = 0.15$) centered at the jet mo-

mentum direction with the transverse energy deposit to this small cone more than 0.95 of the jet. The second method could tag the τ decay into 2π and 3π originated from $\tau \rightarrow \rho\nu$ and $a_1\nu$ decays, in addition to the single π . Thus the tagging efficiency is better than the first method, but the spin analysis power is weakened.

The extensive signal-to-background studies including τ 's can be found, for example, in Ref. [13,14]. Following their results, a clear signal extraction is expected by the requirement of the same-signed dilepton and possibly a peak in their invariant-mass. Thus, we present the simulation results only for the signal events, but not for the background events. Expected background processes are diboson production, $t\bar{t}$ plus one boson production, etc.

As the first case, we deal with $pp \rightarrow H^{++}H^{--} \rightarrow \ell^+\ell^+\ell^-\tau^-$. This decay pattern can be easily identified by requiring the same-signed dilepton with a sharp peak in their invariant-mass distribution. The mass of $H^{\pm\pm}$ can be clearly obtained from the peak. Then, the invariant-mass distribution of the remaining ℓ^- and decay products of τ^- can be used for the polarization discriminator. We take the hadronic decays of τ , because of the better spin analysis power than the leptonic ones as shown in Fig. 1.

In Fig. 3, the invariant-mass distributions of $\ell\pi\tau$ (left panel) and those of ℓj_τ (right panel) from $H^{--} \rightarrow \ell^-\tau^-$ are shown for the events with 3ℓ and one τ -tagged jet. Results for the decay of $H_L^{\pm\pm}$ ($H_R^{\pm\pm}$) are plotted in the dashed (solid) histograms. The y -axis of the plots hereafter stands for the number of events in our simulation. For each of $H_L^{\pm\pm}$ and $H_R^{\pm\pm}$, we generate 3×10^4 events of the $pp \rightarrow H^{++}H^{--} \rightarrow \ell^+\ell^+\ell^-\tau^-$ process followed only by hadronic τ decays. Corresponding integrated luminosity of our simulation depends on the branching ratio of $H^{\pm\pm}$, which however we don't specify in this study. The signal selection efficiencies with the π_τ method and the j_τ method in Fig. 3 are about 13% (15%) and 62% (62%), for $H_L^{\pm\pm}$ ($H_R^{\pm\pm}$) events in our simulation, respectively.

The distributions in the left panel roughly reproduce the linear dependence on z given in Eqs. (4) which are superimposed with some normalization. Thus, the pionic τ -tagging method seems to be working well to catch the pionic τ decay products. The effect of the kinematical cuts can appear in the small z region due to the p_T cut. The discrimination of the two distributions may be possible with just a small number of events. When we employ the general τ -tagging method, the expected number of events becomes 5 times larger than that for the case with pionic τ -tagging method. Since the distributions for $H_L^{\pm\pm}$ and $H_R^{\pm\pm}$ still differ from each other, although the difference is weakened, this general τ -tagging method works as well for our purpose. We note that the distributions in the right panel could be understood as the sum of the various hadronic τ decay contributions with proper polarization

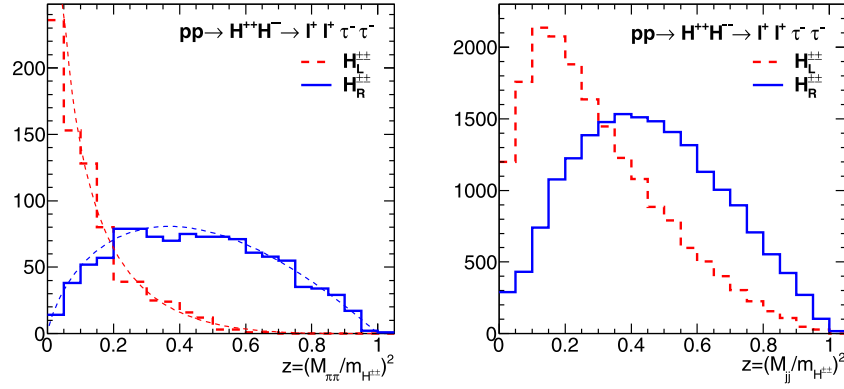


Fig. 4. Invariant-mass distributions of $\pi_{\tau}\pi_{\tau}$ (left) and $j_{\tau}j_{\tau}$ (right) in the $pp \rightarrow H^{++}H^{-} \rightarrow \ell^{+}\ell^{+}\tau^{-}\tau^{-}$ process followed by hadronic decays of τ 's, after the requirement of the same-signed dilepton with $M_{\ell\ell} \simeq m_{H^{\pm\pm}}$. Dashed (solid) histograms are for $H_L^{\pm\pm}$ ($H_R^{\pm\pm}$). Smooth lines in the left panel are theoretical expectations by using Eqs. (6) with some normalization.

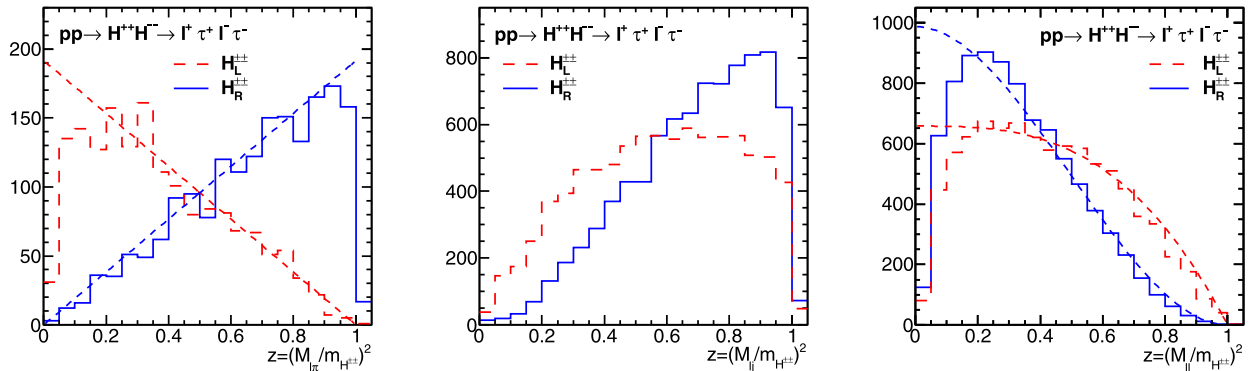


Fig. 5. Invariant-mass distributions of $\ell\pi_{\tau}$ (left), ℓj_{τ} (middle) and $\ell\ell_{\tau}$ (right) in the $pp \rightarrow H^{++}H^{-} \rightarrow \ell^{+}\tau^{+}\ell^{-}\tau^{-}$ process followed by one leptonic and one hadronic decays of τ 's after the requirement of the proper momentum reconstruction by using the collinear approximation method. Dashed (solid) histograms are for $H_L^{\pm\pm}$ ($H_R^{\pm\pm}$). Smooth lines in the left and right panels are theoretical expectations by using Eqs. (4) and Eqs. (5), respectively, with some normalization.

dependence [19]. The distributions are scaled by the mass of $H^{\pm\pm}$, thus it is expected that these distributions does not depend on the value of the mass so much. We have confirmed that quite similar distributions are obtained for the case with a heavier mass of $H^{\pm\pm}$.

The second case is $pp \rightarrow H^{++}H^{-} \rightarrow \ell^{+}\ell^{+}\tau^{-}\tau^{-}$. We note that this process can be useful when the branching ratio for the LFV decay $H^{-} \rightarrow \ell^{-}\tau^{-}$ is so small that we cannot use the first case ($H^{++}H^{-} \rightarrow \ell^{+}\ell^{+}\ell^{-}\tau^{-}$). This collider signature has also a sharp peak in the invariant-mass distribution of the same-signed dilepton, thus the signal event extraction from the background contributions would be easy. We analyze the case where both of τ leptons decay into hadrons because of the best spin analysis power as shown in Fig. 2.

In Fig. 4, the invariant-mass distributions of $\pi_{\tau}\pi_{\tau}$ (left panel) and those of $j_{\tau}j_{\tau}$ (right panel) from $H^{-} \rightarrow \tau^{-}\tau^{-}$ in the $pp \rightarrow H^{++}H^{-} \rightarrow \ell^{+}\ell^{+}\tau^{-}\tau^{-}$ process are shown. We generate 3×10^4 events of the process followed only by the hadronic decays of τ 's. Results for the decay of $H_L^{\pm\pm}$ ($H_R^{\pm\pm}$) are plotted in the dashed (solid) histograms. Distributions of Eqs. (6) are superimposed to the left panel with some normalization as references. As expected, behaviors of the distributions in the left panel are almost the same as Eqs. (6) even after the selection cuts. For the $j_{\tau}j_{\tau}$ invariant-mass distributions, the curves for $H_L^{\pm\pm}$ and for $H_R^{\pm\pm}$ are still well separated.

The third case is for a situation in which $H^{-} \rightarrow \ell^{-}\ell^{-}$ does not exist. Then the signature would be $pp \rightarrow H^{++}H^{-} \rightarrow \ell^{+}\tau^{+}\ell^{-}\tau^{-}$, which seems better than $pp \rightarrow H^{++}H^{-} \rightarrow \ell^{+}\tau^{+}\tau^{-}\tau^{-}$. The momentum reconstruction of the two τ 's is still possible by using a

collinear approximation for the decay of the two τ 's [13]. Then the mass of $H^{\pm\pm}$ can be measured by the invariant-mass of the same-signed $\ell\tau$ pairs. If both of the τ 's decay hadronically, we may suffer from the background contribution. In order to suppress the background contribution, we require that one τ decays leptonically which gives the same-signed dilepton $\ell\ell_{\tau}$. The hadronic decay for the other τ will be preferred for the discrimination of the polarization, although the $\ell^{+}\ell_{\tau}^{+}\ell^{-}\ell_{\tau}^{-}$ signature may be also exploited.

In Fig. 5, the invariant-mass distributions of $\ell\pi_{\tau}$ (left panel), those of ℓj_{τ} (middle panel) are shown for the event in which the momentum reconstruction is resolved by using the collinear approximation method.⁴ We generate 3×10^4 events of the $pp \rightarrow H^{++}H^{-} \rightarrow \ell^{+}\tau^{+}\ell^{-}\tau^{-}$ process. The decay of a tau lepton is not restricted to the hadronic ones in contrast with simulations for Figs. 3 and 4. The full momentum reconstruction is not necessary to obtain the plots in Fig. 5, but is very effective to extract the signal events of this decay pattern. Distributions of Eqs. (6) are superimposed to the left panel with some normalization as references. Behaviors of the obtained invariant-mass distributions of $\ell\pi_{\tau}$ and ℓj_{τ} are almost the same as those in the $pp \rightarrow H^{++}H^{-} \rightarrow \ell^{+}\ell^{+}\ell^{-}\tau^{-}$ process in Fig. 3. In addition, in the right panel, we plot the invariant-mass distributions of the same-signed $\ell\ell_{\tau}$ pair from the other side of the $H^{\pm\pm}$ decays. The behaviors

⁴ One may wonder how to select ℓ_{τ}^{-} for the collinear approximation method under the existence of ℓ^{-} . One can find the correct one which gives the smaller difference of the reconstructed invariant-masses of the two $\ell^{\pm}\tau^{\pm}$ pairs.

of $\ell\ell_\tau$ invariant-mass distributions are in good agreement with Eqs. (5) whose distributions are superimposed with some normalization as references. Due to the good momentum resolution of leptons, the dilepton invariant-mass distributions could be also useful for the τ polarization discrimination.

Finally, we comment on the case where H^{--} decays only into $\ell^-\ell^-$ or $\tau^-\tau^-$. If H^{--} decays only into $\ell^-\ell^-$, it is impossible to observe any polarization phenomena from kinematical measurements. Then we should rely on predictions in each model about the $H^{\pm\pm}$ production cross-section and the decay branching ratios in order to distinguish models. If H^{--} decays only into $\tau^-\tau^-$, $H^{++}H^{--}$ gives the 4τ signature. Since, there are too many sources of the missing momentum, the momentum reconstruction for the τ 's is not possible, we cannot use the invariant-mass peak at $m_{H^{\pm\pm}}$ for the background reduction. For the similar signatures in the context of the two Higgs doublet model, however, a sufficient background reduction is expected in the various channels for the τ decays [28]. Thus, the invariant-mass distributions, for example, in the $\ell^\pm\ell_\tau^\pm j_\tau j_\tau$ channel may be used for the polarization discriminant. Notice that the information on $m_{H^{\pm\pm}}$ could be obtained by the endpoint of the invariant-mass distributions [28].

4. Conclusions

The doubly charged scalar boson $H^{\pm\pm}$ appears in several new physics models, especially in the models to generate Majorana neutrino masses. The $H^{\pm\pm}$ has characteristic Yukawa interactions with two *left-handed* charged leptons (e.g., $\Delta^{\pm\pm}$ from an $SU(2)_L$ triplet field in the HTM) or two *right-handed* charged leptons (e.g., $k^{\pm\pm}$ from an $SU(2)_L$ singlet field in the ZBM) depending on the model. We have studied the kinematical consequences of the Yukawa interactions in order to discriminate these models through the determination of the chiral structure of the Yukawa interaction.

At collider experiments, it is known that the polarization of the τ lepton is analyzed by the energy fraction distributions of its decay products (π^\pm , ℓ^\pm , etc.). We have seen that the invariant-mass distributions are good analyzers of the τ polarization especially for the hadronic τ decays.

We have performed a simple Monte-Carlo simulation for decays of τ 's made from the decays of pair-produced $H^{\pm\pm}$. If $H^{++}H^{--} \rightarrow \ell^+\ell^+\ell^-\ell^-$ mode exists ($\ell = e, \mu$), the invariant-mass distribution of $\ell^-\ell^-$ gives the best analysis power on τ polarization. The background contribution can be highly reduced by requiring $\ell^+\ell^+$ whose invariant-mass is $\simeq m_{H^{\pm\pm}}$. We have shown that $H^{++}H^{--} \rightarrow \ell^+\ell^+\tau^-\tau^-$ mode followed by $\tau \rightarrow \pi\nu$ for both τ is also useful to discriminate the τ polarization by using the distribution of the invariant-mass of $\pi_\tau\pi_\tau$. Even if there is no $H^{++} \rightarrow \ell^+\ell^+$, we have found that τ polarization can be determined by the distribution of the invariant-mass $M_{\ell\pi_\tau}$ in $H^{++}H^{--} \rightarrow \ell^+\tau^+\ell^-\tau^-$ mode with a leptonic and a pionic τ decays. The reduction of the background events can be achieved by requiring same-signed $\ell\ell_\tau$ with the collinear approximation method. Therefore, in these various cases for the leptonic decay of $H^{\pm\pm}$, we can determine the chiral structure of the Yukawa interaction of $H^{\pm\pm}$, and it will help to discriminate new physics models beyond the SM.

Acknowledgements

The work of H.S. was supported in part by the Grant-in-Aid for Young Scientists (B) No. 23740210. The work of K.T. was supported, in part, by the Grant-in-Aid for Scientific research from the

Ministry of Education, Science, Sports, and Culture (MEXT), Japan, No. 23104011. The work of H.Y. was supported in part by the National Science Council of Taiwan under Grant No. NSC 100-2119-M-002-001.

References

- [1] B.T. Cleveland, et al., *Astrophys. J.* 496 (1998) 505; W. Hampel, et al., GALLEX Collaboration, *Phys. Lett. B* 447 (1999) 127; B. Aharmim, et al., SNO Collaboration, *Phys. Rev. Lett.* 101 (2008) 111301; J.N. Abdurashitov, et al., SAGE Collaboration, *Phys. Rev. C* 80 (2009) 015807; K. Abe, et al., Super-Kamiokande Collaboration, *Phys. Rev. D* 83 (2011) 052010; G. Bellini, et al., Borexino Collaboration, *Phys. Rev. Lett.* 107 (2011) 141302.
- [2] R. Wendell, et al., Kamiokande Collaboration, *Phys. Rev. D* 81 (2010) 092004.
- [3] M.H. Ahn, et al., K2K Collaboration, *Phys. Rev. D* 74 (2006) 072003; P. Adamson, et al., The MINOS Collaboration, *Phys. Rev. Lett.* 106 (2011) 181801.
- [4] K. Abe, et al., T2K Collaboration, *Phys. Rev. Lett.* 107 (2011) 041801.
- [5] M. Apollonio, et al., CHOOZ Collaboration, *Eur. Phys. J. C* 27 (2003) 331; Y. Abe, et al., DOUBLE-CHOOZ Collaboration, *Phys. Rev. Lett.* 108 (2012) 131801; F.P. An, et al., DAYA-BAY Collaboration, *Phys. Rev. Lett.* 108 (2012) 171803; J.K. Ahn, et al., RENO Collaboration, *Phys. Rev. Lett.* 108 (2012) 191802.
- [6] A. Gando, et al., KamLAND Collaboration, *Phys. Rev. D* 83 (2011) 052002.
- [7] E. Majorana, *Nuovo Cim.* 14 (1937) 171.
- [8] W. Konetschny, W. Kummer, *Phys. Lett. B* 70 (1977) 433; M. Magg, C. Wetterich, *Phys. Lett. B* 94 (1980) 61; T.P. Cheng, L.F. Li, *Phys. Rev. D* 22 (1980) 2860; J. Schechter, J.W.F. Valle, *Phys. Rev. D* 22 (1980) 2227.
- [9] R.N. Mohapatra, G. Senjanovic, *Phys. Rev. Lett.* 44 (1980) 912; G. Lazarides, Q. Shafi, C. Wetterich, *Nucl. Phys. B* 181 (1981) 287; N. Arkani-Hamed, A.G. Cohen, E. Katz, A.E. Nelson, *JHEP* 0207 (2002) 034.
- [10] A. Zee, *Nucl. Phys. B* 264 (1986) 99; K.S. Babu, *Phys. Lett. B* 203 (1988) 132.
- [11] M. Aoki, S. Kanemura, K. Yagyu, *Phys. Lett. B* 702 (2011) 355; M. Aoki, S. Kanemura, K. Yagyu, *Phys. Lett. B* 706 (2012) 495 (Erratum); B. Ren, K. Tsumura, X.-G. He, *Phys. Rev. D* 84 (2011) 073004.
- [12] A.G. Akeroyd, M. Aoki, *Phys. Rev. D* 72 (2005) 035011; A.G. Akeroyd, C.-W. Chiang, *Phys. Rev. D* 80 (2009) 113010; A.G. Akeroyd, C.-W. Chiang, N. Gaur, *JHEP* 1011 (2010) 005.
- [13] A. Hektor, M. Kadastik, M. Muntel, M. Raidal, L. Rebane, *Nucl. Phys. B* 787 (2007) 198.
- [14] P. Fileviez Perez, T. Han, G.-y. Huang, T. Li, K. Wang, *Phys. Rev. D* 78 (2008) 015018; C.-W. Chiang, T. Nomura, K. Tsumura, *Phys. Rev. D* 85 (2012) 095023.
- [15] D. Acosta, et al., CDF Collaboration, *Phys. Rev. Lett.* 93 (2004) 221802; D. Acosta, et al., CDF Collaboration, *Phys. Rev. Lett.* 95 (2005) 071801; T. Aaltonen, et al., CDF Collaboration, *Phys. Rev. Lett.* 101 (2008) 121801; V.M. Abazov, et al., D0 Collaboration, *Phys. Rev. Lett.* 93 (2004) 141801; V.M. Abazov, et al., *Phys. Rev. Lett.* 101 (2008) 071803; V.M. Abazov, et al., *Phys. Rev. Lett.* 108 (2012) 021801.
- [16] CMS Collaboration, CMS PAS HIG-12-005, March 2011.
- [17] G. Aad, et al., ATLAS Collaboration, *Phys. Rev. D* 85 (2012) 032004.
- [18] A.G. Akeroyd, H. Sugiyama, *Phys. Rev. D* 84 (2011) 035010; M. Aoki, S. Kanemura, K. Yagyu, *Phys. Rev. D* 85 (2012) 055007; A.G. Akeroyd, S. Moretti, H. Sugiyama, *Phys. Rev. D* 85 (2012) 055026.
- [19] B.K. Bullock, K. Hagiwara, A.D. Martin, *Phys. Rev. Lett.* 67 (1991) 3055; B.K. Bullock, K. Hagiwara, A.D. Martin, *Phys. Lett. B* 273 (1991) 501; B.K. Bullock, K. Hagiwara, A.D. Martin, *Nucl. Phys. B* 395 (1993) 499.
- [20] M.M. Nojiri, *Phys. Rev. D* 51 (1995) 6281; M.M. Nojiri, K. Fujii, T. Tsukamoto, *Phys. Rev. D* 54 (1996) 6756.
- [21] S.Y. Choi, K. Hagiwara, Y.G. Kim, K. Mawatari, P.M. Zerwas, *Phys. Lett. B* 648 (2007) 207.
- [22] E.J. Chun, K.Y. Lee, S.C. Park, *Phys. Lett. B* 566 (2003) 142; J. Garayoa, T. Schwetz, *JHEP* 0803 (2008) 009; A.G. Akeroyd, M. Aoki, H. Sugiyama, *Phys. Rev. D* 77 (2008) 075010; M. Kadastik, M. Raidal, L. Rebane, *Phys. Rev. D* 77 (2008) 115023.
- [23] K.L. McDonald, B.H.J. McKellar, hep-ph/0309270.
- [24] M. Nebot, J.F. Oliver, D. Palao, A. Santamaria, *Phys. Rev. D* 77 (2008) 093013.
- [25] T. Sjostrand, S. Mrenna, P.Z. Skands, *JHEP* 0605 (2006) 026.
- [26] S. Jadach, Z. Was, R. Decker, J.H. Kuhn, *Comput. Phys. Commun.* 76 (1993) 361.
- [27] M. Cacciari, G.P. Salam, G. Soyez, *JHEP* 0804 (2008) 063.
- [28] S. Kanemura, K. Tsumura, H. Yokoya, *Phys. Rev. D* 85 (2012) 095001.